iScience

CellPress
OPEN ACCESS

Article

AKAP150 from nucleus accumbens dopamine D1 and D2 receptor-expressing medium spiny neurons regulates morphine withdrawal

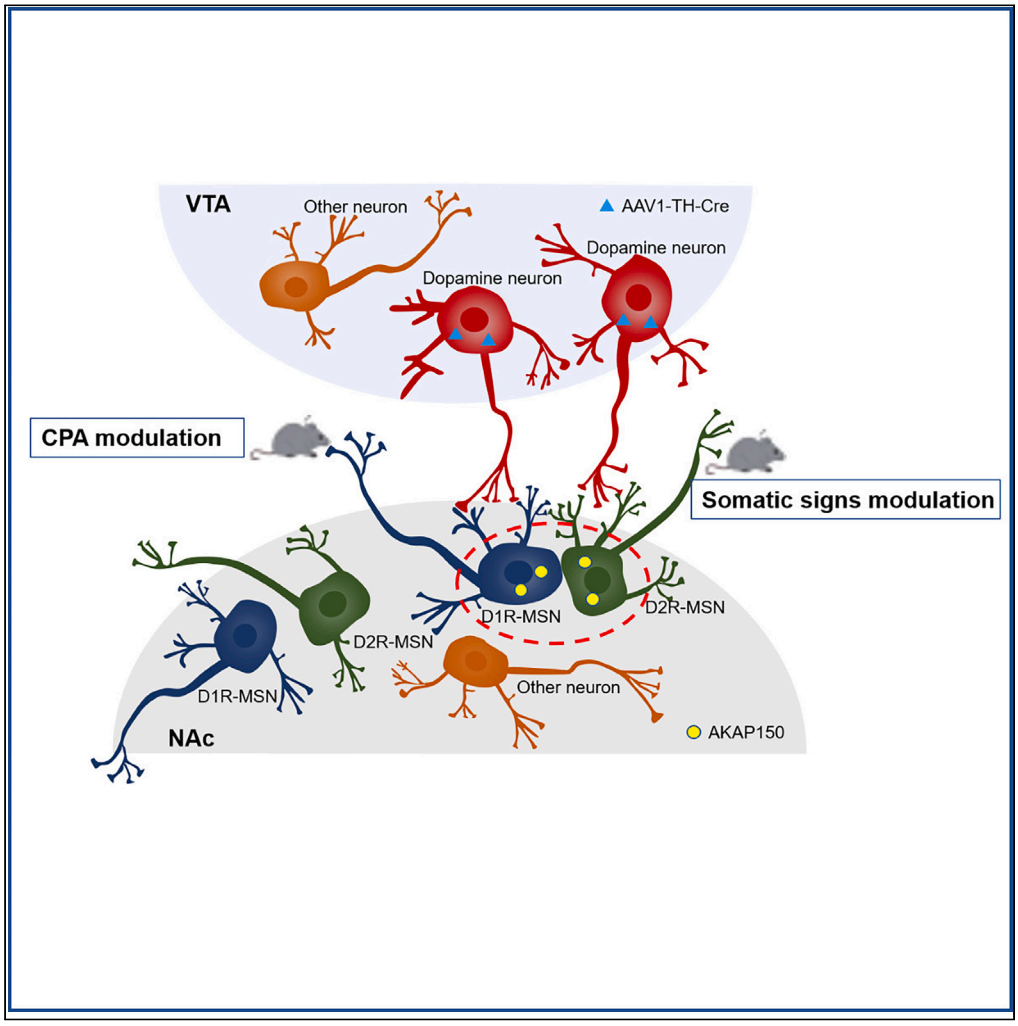

Xiaohui Bai, Kun Zhang, Chaopeng Ou, ..., Yingjun Zhang, Wan Huang, Handong Ouyang

zhangyingj@sysucc.org.cn (Y.Z.)
huangwan@sysucc.org.cn (W.H.)
ouyhd@sysucc.org.cn (H.O.)

Highlights

Knockdown of AKAP150 in NAc relieved morphine withdrawal somatic response and CPA

NAc D1R-MSNs and D2R-MSNs played different roles in the process of morphine withdrawal

Expression of AKAP150 in NAc was mediated by signal from VTA

Bai et al., iScience *26*, 108227
November 17, 2023
https://doi.org/10.1016/j.isci.2023.108227

iScience

CellPress
OPEN ACCESS

Article

AKAP150 from nucleus accumbens dopamine D1 and D2 receptor-expressing medium spiny neurons regulates morphine withdrawal

Xiaohui Bai,[1,2,3] Kun Zhang,[1,3] Chaopeng Ou,[1,3] Yanyu Mu,[1,3] Dongmei Chi,[1] Jianxing Zhang,[1] Jingxiu Huang,[1] Xile Li,[1] Yingjun Zhang,[1,*] Wan Huang,[1,*] and Handong Ouyang[1,4,*]

SUMMARY

Dopamine D1 receptor-expressing medium spiny neurons (D1R-MSNs) and dopamine D2 receptor-expressing MSNs (D2R-MSNs) in nucleus accumbens (NAc) have been demonstrated to show different effects on reward and memory of abstinence. A-kinase anchoring protein 150 (AKAP150) expression in NAc is significantly upregulated and contributes to the morphine withdrawal behavior. However, the underlying mechanism of AKAP150 under opioid withdrawal remains unclear. In this study, AKAP150 expression in NAc is upregulated in naloxone-precipitated morphine withdrawal model, and knockdown of AKAP150 alleviates morphine withdrawal somatic signs and improves the performance of conditioned place aversion (CPA) test. AKAP150 in NAc D1R-MSNs is related to modulation of the performance of morphine withdrawal CPA test, while AKAP150 in NAc D2R-MSNs is relevant to the severity of somatic responses. Our results suggest that AKAP150 from D1R-MSNs or D2R-MSNs in NAc contributes to the developmental process of morphine withdrawal but plays different roles in aspects of behavior or psychology.

INTRODUCTION

Morphine is a powerful analgesic and also an addictive drug due to its powerful euphoria-inducing effects.[1] Opioid abuse has had a detrimental impact on both the families of affected individuals and society as a whole, making it a pressing global health concern that requires immediate solutions.[2] The rewarding effects of the drug and the reluctance to experience withdrawal signs motivate repetitive drug use.[3] Repeated administration of opioids results in physical dependence and conditioning. Besides, opiate withdrawal syndromes, such as pain, agitation, sleep disturbances, and anxiety, counterbalance the benefits of opiates in human.[4,5] In opioid-addicted rodents or mice, naloxone can induce opiate abstinence syndromes such as wet-dog shake, jumping, paw tremor, teeth chattering, which is a recognized paradigm of negative affective learning.[6,7] Therefore, elucidating the mechanism modulating the negative affective states during opiate withdrawal should be essential in solving drug addiction as well as relapse.

The brain's reward pathway, especially the mesocorticolimbic dopamine system, has been found to be involved in opioid addiction.[8,9] The most significant component of the mesocorticolimbic dopamine system is the projecting neurons that connect the ventral tegmental area (VTA) and nucleus accumbens (NAc).[10] Opioids regulate opioid receptors and the firing of dopamine neurons, and dopamine neurotransmission in the VTA and NAc, which can modulate the rewarding and reinforcing effects of drugs. Other addictive substances also increase dopamine concentrations in the NAc, which is why the NAc is a potential therapeutic target for the treatment of opioid addiction.[11] The NAc has been shown to play a crucial role in the development of opioid addiction,[12] but its role in opiate withdrawal is not yet fully understood.

The signaling complex of postsynaptic scaffolding A-kinase anchoring protein 79/150 (AKAP79/150, human AKAP79/bovine150) regulates excitatory synaptic transmission and strength by targeting protein kinase A (PKA), protein kinase C (PKC), and calcineurin (CaN) to the postsynaptic densities of neurons.[13] AKAP150 is a postsynaptic scaffolding protein that can integrate signals by binding various signaling, scaffolding, receptor, and ion channel proteins involved in long-term synaptic plasticity.[14] Previous evidence has shown that AKAP150 increases the NAc postsynaptic density of cocaine-treated rats, and disruption of AKAP-dependent signaling in the NAc attenuates cocaine reinstatement.[15] Therefore, AKAP in the NAc could be an effective therapeutic target for drug addiction.

[1]Department of Anesthesiology, State Key Laboratory of Oncology in South China, Guangdong Provincial Clinical Research Center for Cancer, Sun Yat-sen University Cancer Center, Guangzhou, P.R. China
[2]Department of Anesthesiology, Guangdong Provincial Key Laboratory of Malignant Tumor Epigenetics and Gene Regulation, Sun Yat-sen Memorial Hospital, Sun Yat-sen University, Guangzhou, China
[3]These authors contributed equally
[4]Lead contact
*Correspondence: zhangyingj@sysucc.org.cn (Y.Z.), huangwan@sysucc.org.cn (W.H.), ouyhd@sysucc.org.cn (H.O.)
https://doi.org/10.1016/j.isci.2023.108227

The circuit connecting the VTA and NAc has a significant impact on the development of drug addiction.[16,17] Most of the rewarding/aversive signals from the VTA are dopaminergic and act through two distinct neuronal populations of GABAergic medium spiny neurons (MSNs), which are divided into dopamine D1 receptor (D1R)-expressing MSNs (D1R-MSNs) and dopamine D2 receptor (D2R)-expressing MSNs (D2R-MSNs).[18,19] D1R- and D2R-MSNs have been considered to have different functions in the process of opioid addiction. Previous studies have showed that activation of D1R-MSNs is related to positive rewarding events, while D2R-MSNs signaling mediate aversion.[20,21] Lobo et al.[20] reported that activation of D1 neurons results in enhancement of conditioned place preference, whereas activation of D2 neurons attenuates preference. And Kravitz et al.[21] found that activation of D1R-MSNs causes positive responses to rewarding stimuli, while activation of D2R-MSNs induces aversion and suppression of reward or motivated behavior in both place preference and operant tasks. However, not all research results are completely consistent. Another research indicated that both D1 and D2 neurons in the NAc contribute in the same direction in the modulation of motivation, and activation of either neuronal population enhances motivation in mice. There should be a more complex relationship between D1R- and D2R-MSNs in the NAc, since putative D1 neurons can drive behavioral aversion, while D2 neurons' stimulation can increase reward seeking in certain conditions.[22] And tyrosine hydroxylase (TH) is one of the main factors that regulate and mediate the dopamine neurons between VTA and NAc.[23] To better elucidate the role of NAc AKAP150 in the process of morphine addiction and morphine withdrawal, this study aims to explore the function of AKAP150 in the NAc using morphine withdrawal mice and explored the different functions of subpopulation AKAP150 in D1R- and D2R-MSNs in the morphine withdrawal-induced aversion and somatic signs. And we further investigated the impact of dopamine neuron from VTA on the regulation of NAc AKAP150 to uncover the underlying mechanism. We aim to better elucidate the mechanism of morphine withdrawal and identify specific targets to inhibit morphine withdrawal syndrome and solve morphine addiction.

RESULTS

AKAP150 was upregulated in the NAc in morphine withdrawal-induced CPA model

We tested the effectiveness of our morphine withdrawal-induced CPA model and examined changes of AKAP150 in the NAc (Figure 1). Mice that suffered from morphine withdrawal were found to have more involuntary movements; including jumps, paw tremor, teeth chattering, wet-dog shake, diarrhea, and loss of body weight (Figure 1D). The morphine withdrawal score was significantly higher in morphine withdrawal group than in control group. After the morphine withdrawal CPA model was established, the mice spent significantly less time in the paired compartment and the aversion score was significantly reduced in morphine withdrawal CPA model (Figure 1E). The movement of all mice did not significantly change before and after CPA test (Figure 1F). These data showed that the CPA model was successfully established. The PCR, immunohistochemical staining (IHC), and western blot results showed that AKAP150 mRNA and protein expression in the NAc increased significantly in the morphine withdrawal CPA model (Figures 1G–1I). The expression of c-fos in NAc was upregulated after morphine withdrawal, implying activation of neurons in the region (Figure 1J). And the density of dendritic spine was significantly higher in morphine withdrawal group (Figure 1K). We speculate that upregulation of AKAP150 expression might be relevant to the development of aversion.

Knockdown of AKAP150 expression relieved morphine withdrawal somatic response and CPA

We examined changes in behavior and tissue after knockdown of AKAP150 expression in the NAc. The knockdown efficiency is shown in Figure S3A. After we knocked down the expression of AKAP150 in WT mice, the observed involuntary movements including jumps, paw tremor, teeth chattering, wet-dog shake, diarrhea, and loss of body weight (%) were decreased after morphine withdrawal (Figure 2A). The morphine withdrawal score was significantly lower (Figure 2A), and the aversion score was higher in WT mice with knock downing expression of AKAP150 (Figure 2B). Result of c-fos showed that expression of c-fos was obviously reduced after AKAP150 knockdown (Figure 2C). As for the density of dendritic spines, the density was significantly reduced after AKAP150 knockdown (Figure 2D).

We carried out similar experiment in AKAP150 $^{fl/fl}$ mice. We stereotaxically injected AAV-CMV-Cre-EGFP and the corresponding control virus (Table 1) into the NAc to conditionally knock down the expression of AKAP150 in AKAP150 $^{fl/fl}$ mice. Similar results were found. The knockdown efficiency is shown in Figure S3B. When conditionally knocking down the expression of AKAP150 in the NAc of AKAP150 $^{fl/fl}$ mice, the morphine withdrawal score gained lower (Figure 3A), and the aversion score was higher (Figure 3B). Expression of c-fos was obviously reduced after AKAP150 knockdown in AKAP150 $^{fl/fl}$ mice (Figure 3C). And density of dendritic spine was decreased after AKAP150 knockdown in AKAP150 $^{fl/fl}$ mice (Figure 3D).

These results show that knockdown of AKAP150 expression is beneficial for alleviating naloxone-precipitated morphine withdrawal somatic response. Meantime, knockdown of AKAP150 expression in NAc relieves morphine withdrawal CPA. It might be evidence that AKAP150 participates in the process of morphine withdrawal through stimulation of neuron activity and regulation of dendritic spines' density.

AKAP150 was highly expressed in D1R-MSNs and D2R-MSNs in NAc

To explore cell-type-specific change after opioid injection, we reanalyzed single-cell RNA sequencing (scRNA-seq) data (GEO: GSE118918) from a study investigating the transcriptional response of NAc of mice to acute morphine treatment.[24] A total of 35,878 cell transcriptomes were retained for subsequent analysis and were annotated into 19 major cell types based on the expression of the most variable genes and their canonical markers, consistent with the original paper[24] (Figures 4A and S1A–S1C; Table S1). Our reanalysis revealed the gene of AKAP150 was specifically high expressed in D1R-MSN, D2R-MSN, and GABA other clusters at single cell resolution (Figures 4B and 4C). Next, we compared expression of AKAP150 between morphine- and saline-treated group in afore-mentioned three clusters separately

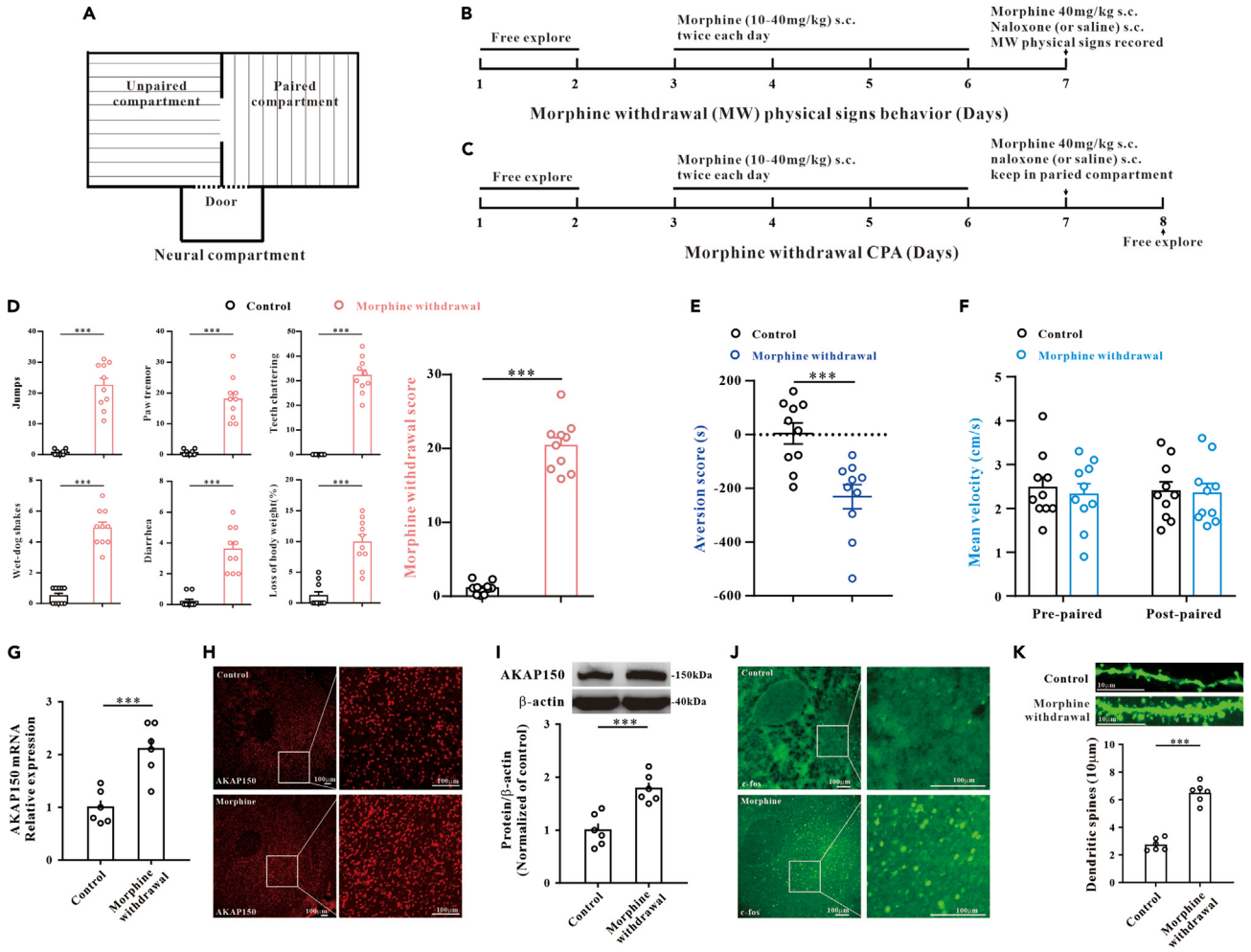

Figure 1. Expression of AKAP150 upregulated in the NAc after naloxone-precipitated morphine withdrawal

(A–C) Schematic of the three-compartment apparatus applied for the CPA test. (B and C) Experimental timeline of the morphine withdrawal physical signs test (B) and the morphine withdrawal CPA model (C).

(D) Morphine withdrawal physical signs test [jumps (***P<0.001, Mann-Whitney U test, n = 10), paw tremor (***P<0.001, Mann-Whitney U test, n = 10), teeth chattering (***P<0.001, Mann-Whitney U test, n = 10), wet-dog shake (***P<0.001, Mann-Whitney U test, n = 10), diarrhea (***P<0.001, Mann-Whitney U test, n = 10), and loss of body weight (***P<0.001, Mann-Whitney U test, n = 10)] and morphine withdrawal score (***P<0.001, t test, n = 10) was significantly increased after morphine withdrawal in WT mice.

(E) Less time was spent in the paired compartment after the morphine withdrawal CPA model was established. CPA aversion score was significantly reduced after morphine withdrawal in WT mice (***P<0.001, t test, n = 10).

(F) Mean velocity showed no significant difference before and after morphine withdrawal (Pre-paired, p = 0.6961, t test; Post-paired, p = 0.7676, t test; n = 10).

(G–I) AKAP150 mRNA (G) and protein expression (H and I) were upregulated in morphine withdrawal model by PCR, IHC, and WB test (***P<0.001, t test, n = 6).

(J). IHC showing c-fos expression was upregulated after morphine withdrawal. Scale bar, 100μm.

(K) Representative images of GFP-labeled dendrites and the statistical data for density of dendritic spines, demonstrating the density of dendritic spine was significantly higher after morphine withdrawal (***P<0.001, t test, n = 6). Data are shown as the mean ± SEM.

and found that the AKAP150 expression was not increased in the group with acute morphine treatment (Figure 4D). Our PCR results showed that AKAP150 mRNA relative expression was not significantly changed in mice with one-time treatment of morphine than those with saline (4 h harvest after morphine injection) (Figure 4E). To directly demonstrate the co-expression of AKAP150 in DIR-MSNs and D2R-MSNs, we ran the IHC test in the naloxone-precipitated morphine withdrawal mice and the results showed that AKAP150 was highly co-expressed in both D1R-MSNs and D2R-MSNs (Figures 4F and 4G).

D1R-MSNs and D2R-MSNs played different roles in the process of naloxone-precipitated morphine withdrawal

We evaluated the role of D1R-MSNs and D2R-MSNs' AKAP150 in the process of naloxone-precipitated morphine withdrawal. We selectively knocked down the expression of AKAP150 in D1R-MSNs or D2R-MSNs in NAc by injecting AAV-D1-Cre along with

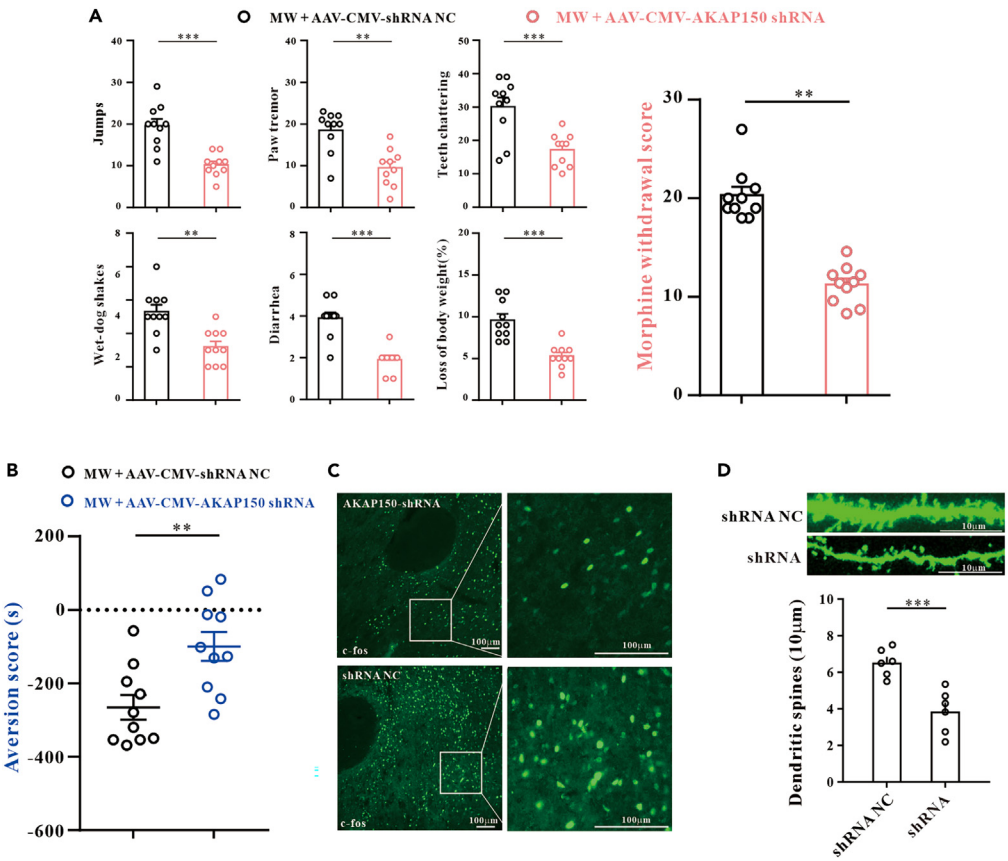

Figure 2. Knockdown of AKAP150 expression in the NAc relieved morphine withdrawal somatic response and CPA score in WT mice

(A) Morphine withdrawal somatic signs including jumps (***P<0.001, t test, n = 10), paw tremor (**P<0.01, Mann-Whitney U test, n = 10), teeth chattering (***P<0.001, t test, n = 10), wet-dog shake (**P<0.01, t test, n = 10), diarrhea (***P<0.001, Mann-Whitney U test, n = 10), and loss of body weight (***P<0.001, t test, n = 10) were decreased, and morphine withdrawal score (**P<0.01, Mann-Whitney U test, n = 10) was significantly lower after knockdown of AKAP150 expression in NAc in WT mice.

(B) Aversion score was improved after knockdown of AKAP150 expression in NAc in WT mice (**P<0.01, t test, n = 10).

(C) IHC showed c-fos expression was downregulated after knockdown of AKAP150 expression in NAc in WT mice. Scale bar, 100μm.

(D) Density of dendritic spines was significantly decreased after knockdown of AKAP150 expression in NAc in WT mice (***P<0.001, t test, n = 6). Scale bar, 10μm. Data are shown as the mean ± SEM.

AAV-CMV-DIO-AKAP150-shRNA or AAV-D2-Cre along with AAV-CMV-DIO-AKAP150-shRNA (Table 1) into the WT mice's NAc. Simply suppressing the expression of AKAP150 in NAc D1R-MSNs would improve the aversion score (Figure 5B) while did not alleviate the morphine withdrawal somatic signs (Figure 5A). On the contrary, simply knocking down the expression of AKAP150 in NAc D2R-MSNs alleviated the morphine withdrawal somatic signs (Figure 5D) without interfering with the aversion score (Figure 5E). And the density of dendritic spine was significantly lower after the knockdown of AKAP150 in D1R-MSNs (Figure 5C) or D2R-MSNs (Figure 5F).

Similar tests were also conducted in AKAP150 $^{fl/fl}$ mice. We stereotaxically injected AAV-D1-Cre-EGFP or AAV-D2-Cre-EGFP (Table 1) into the NAc to conditionally knock down the expression of AKAP150 in D1R-MSNs or D2R-MSNs of AKAP150 $^{fl/fl}$ mice. Suppressing expression of AKAP150 in NAc D1R-MSNs in AKAP150 $^{fl/fl}$ mice improved the aversion score (Figure 6B) while did not interfere with the morphine withdrawal somatic signs (Figure 6A). On the contrary, knocking down the expression of AKAP150 in NAc D2R-MSNs in AKAP150 $^{fl/fl}$ mice reduced the morphine withdrawal somatic responses (Figure 6D) without interfering with the aversion score (Figure 6E). And the density of dendritic spine was significantly lower after the knockdown of AKAP150 in D1R-MSNs (Figure 6C) or D2R-MSNs (Figure 6F). The IHC images demonstrate double labeling of AKAP150 and D1-MSN or D2-MSN in the AKAP150 $^{fl/fl}$ mice (Figures 6G and 6H).

Expression of AKAP150 in NAc was mediated by signal from VTA

We injected AAV1-TH-Cre into VTA and CMV-DIO-AKAP150-shRNA, D1-DIO-AKAP150-shRNA, or D2-DIO-AKAP150-shRNA (Table 1) into NAc in WT mice to further exploring the effect of naloxone-precipitated morphine withdrawal. The IHC results demonstrated that the projection of TH-Cre across synapse from VTA could activate the expression of D2-DIO-AKAP150-shRNA-EGFP or D2-DIO-AKAP150-shRNA-EGFP in NAc (Figures S2A–S2F). The immunofluorescence images showed that the neurons or axon expressing TH closely surrounded the

Table 1. Viruses used in the study

Virus	Supplier	Cat# No.
rAAV-CMV-AKAP150-shRNA-mCherry	Brain VTA	Special customization
rAAV-CMV- shRNA-NC-mCherry	Brain VTA	Special customization
rAAV-CMV-Cre-EGFP	Brain VTA	PT-0253
rAAV-CMV-EGFP	Brain VTA	PT-0693
rAAV-CMV-DIO-AKAP150-shRNA-mCherry	Brain VTA	Special customization
rAAV-CMV-DIO-shRNA-NC-mCherry	Brain VTA	Special customization
rAAV-D1-Cre-EGFP	Brain VTA	PT-0812
rAAV-D2-Cre-EGFP	Brain VTA	PT-0813
rAAV-D1-EGFP	Brain VTA	PT-0214
rAAV-D2-EGFP	Brain VTA	PT-3245
rAAV-D1-DIO-AKAP150-shRNA-mCherry	Brain VTA	Special customization
rAAV-D1-DIO-shRNA-NC-mCherry	Brain VTA	Special customization
rAAV-D2-DIO-AKAP150-shRNA-mCherry	Brain VTA	Special customization
rAAV-D2-DIO-shRNA-NC-mCherry	Brain VTA	Special customization
AAV1-TH-Cre-EGFP	Brain VTA	PT-0179
rAAV-D1-mCherry	Brain VTA	PT-0757
rAAV-D2-mCherry	Brain VTA	PT-0367
Hysn-FLP: FDIO-EGFP	Brain Case	BC-SL021

D1R-MSNs or D2R-MSNs in the NAc like the pattern of axon connecting with dendritic spine or cell body between neurons (Figures S2G and S2H). And knockdown of AKAP150 in the NAc mediated by VTA would relieve the morphine withdrawal somatic signs (Figure 7A) and improve morphine withdrawal CPA (Figure 7B), with reduced density of dendritic spine (Figure 7C). We used D1-DIO-AKAP150-shRNA to specifically knockdown expression of AKAP150 in D1R-MSNs that were mediated by dopamine neurons in VTA. After morphine withdrawal, the morphine withdrawal aversion was improved (Figure 7D) without relieving or worsening the somatic response (Figure 7E), with reduced density of dendritic spine (Figure 7F). And D2-DIO-AKAP150-shRNA was used to specifically knockdown expression of AKAP150 in D2R-MSNs that were mediated by dopamine neurons in VTA. After morphine withdrawal, the morphine withdrawal somatic signs were alleviated (Figure 7G) but the morphine withdrawal CPA was not improved (Figure 7H), with reduced density of dendritic spine (Figure 7I). These results indicate that expression of AKAP from D1R-MSNs and D2R-MSNs in NAc receives modulation of VTA.

DISCUSSION

In the present study, we demonstrate that level of AKAP150 expression in the NAc is relevant to the severity of morphine withdrawal induced aversion and somatic signs. Activation of neuron activities and higher density of dendritic spine could be found in morphine withdrawal mice. We discover that chronic morphine exposure but not acute morphine exposure increases the gene expression and the protein production of AKAP150 in NAc. Furthermore, we testified the distinctive roles of AKAP150 in D1R- and D2R MSNs. Consistent with this, knockdown of AKAP150 expression in D1R-MSNs of morphine-dependent mice attenuates morphine withdrawal CPA, while knockdown of AKAP150 in D2R-MSNs alleviates morphine withdrawal somatic signs. This unexpected behavioral outcome further supports that AKAP150 in D1R- and D2R-MSNs in the NAc exert different functions in the psychic and physical dependence on morphine, and it may be a novel target to prevent and treat morphine induced addiction.

Role of AKAP150 in morphine withdrawal signs

AKAPs complexes, despite lacking enzyme activity, function as anchoring proteins that facilitate the recruitment of enzymes and substrates to subcellular structures. This recruitment results in a higher efficacy of signaling transduction, similar to other anchoring proteins.[13] Among these isoforms, AKAP150 has been reported to play a significant role in various forms of neuronal plasticity.[25,26] In particular, AKAP150 regulates PKA signaling in the NAc, which is a crucial mediator of the effects of addictive drugs such as drug-seeking behavior.[15,27] Thus, it is not surprising that the expression of AKAP150 within the NAc in morphine withdrawal mice increased dramatically compared to that in the control group in our present study. To further confirm the potential function of AKAP150 in the development of morphine withdrawal symptoms, we injected CMV-AKAP150 shRNA virus directly into the NAc of morphine-addicted mice and found that this manipulation alleviated the somatic symptoms as well as the expression of CPA induced by morphine withdrawal.

It is well renowned that the expression of c-fos by individual neurons can be used as a marker of neuron activation.[3] Evidence shows that c-fos mRNA expression is induced in several brain regions and particularly in the D1R- and D2R neurons in the NAc during morphine

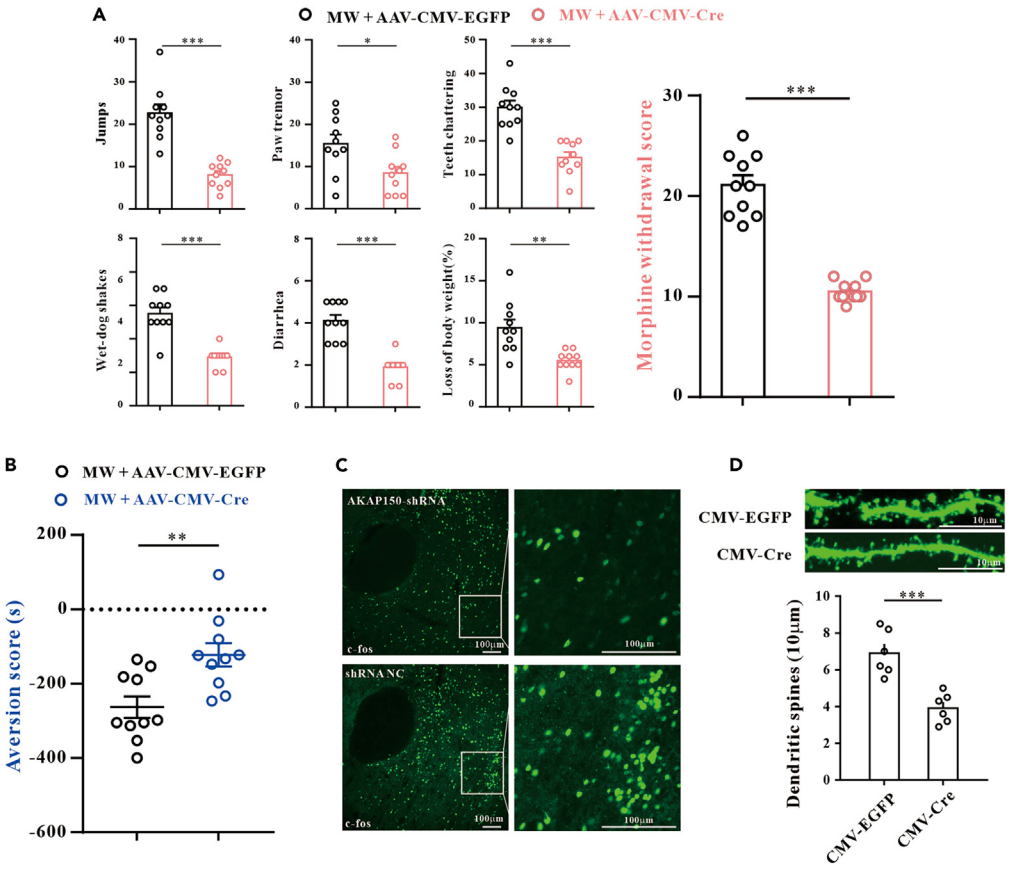

Figure 3. Knockdown of AKAP150 expression in the NAc relieved morphine withdrawal somatic response and aversion score in AKAP150 $^{fl/fl}$ mice

(A) Morphine withdrawal somatic signs including jumps (***P<0.001, t test, n = 10), paw tremor (*P<0.05, t test, n = 10), teeth chattering (***P<0.001, t test, n = 10), wet-dog shake (***P<0.001, Mann-Whitney U test, n = 10), diarrhea (***P<0.001, Mann-Whitney U test, n = 10), and loss of body weight (**P<0.01, t test, n = 10) were decreased, and morphine withdrawal score (***P<0.001, t test, n = 10) was significantly lower after knockdown of AKAP150 expression in NAc in AKAP150 $^{fl/fl}$ mice.

(B) Aversion score was improved after knockdown of AKAP150 expression in NAc in AKAP150 $^{fl/fl}$ mice (**P<0.01, t test, n = 10).

(C) IHC showed c-fos expression was downregulated after knockdown of AKAP150 expression in NAc in AKAP150 $^{fl/fl}$ mice morphine withdrawal model. Scale bar, 100μm.

(D) Density of dendritic spines was significantly decreased after knockdown of AKAP150 expression in NAc in AKAP150 $^{fl/fl}$ mice (***P<0.001, t test, n = 6). Scale bar, 10μm. Data are shown as the mean ± SEM.

withdrawal.[28] In our present study, we used c-fos as a marker for neurons activity, and consistence with the behavior results, the downregulation of AKAP150 directly inhibited c-fos protein expression in morphine addicted mice within the NAc, which indicates that AKAP150 may affect the neuron activity induced by morphine withdrawal. However, in the present study, we only used c-fos as a marker of neuronal activity to examine the activation of MSNs by the conditioned context. Using another marker of neuronal activity such as intercellular calcium to measure the activation of MSNs is needed to confirm this statement.

The literature suggests that chronic morphine exposure leads to significant neuroplastic events, specifically structural and functional changes in the MSNs within the NAc and dopaminergic projections from the VTA, which contribute to the emergence of behavioral symptoms associated with morphine tolerance.[11,29] MSNs are characterized by their high density of dendritic spines, which are crucial structures for the proper function of the central nervous system. Spines are essential components for neuronal connectivity and synaptic plasticity, as they receive inputs from other regions of the brain.[30] And the synaptic plasticity has been recognized as an important mechanism in many nervous system functions.[31] In our present study, we observed that chronic morphine treatment altered the density of dendritic spines in MSNs, which is acknowledged as an indication of synaptic plasticity resulting in addiction-related behaviors.[32,33] And the downregulation of AKAP150 weakened the morphology change of dendritic spines in MSNs induced by morphine withdrawal, which was consistence with the behavior test results. It was previously reported that chronic morphine treatment decreased the density of dendritic spines on NAc MSNs.[34] On the other hand, studies demonstrated that morphine withdrawal reduced spine density in second-order dendritic trunks of NAc shell MSN.[35,36] It seems to be opposite with our results. However, the studies mentioned previously used rats as the experimental animals and the chronic morphine treatment strategy was up to 14 days, while the experimental animals of our study were mice and the administration of morphine only lasted for 5 days, which might affect the results. Besides, in Diana's study,[35] the density of dendritic spines in the NAc shell

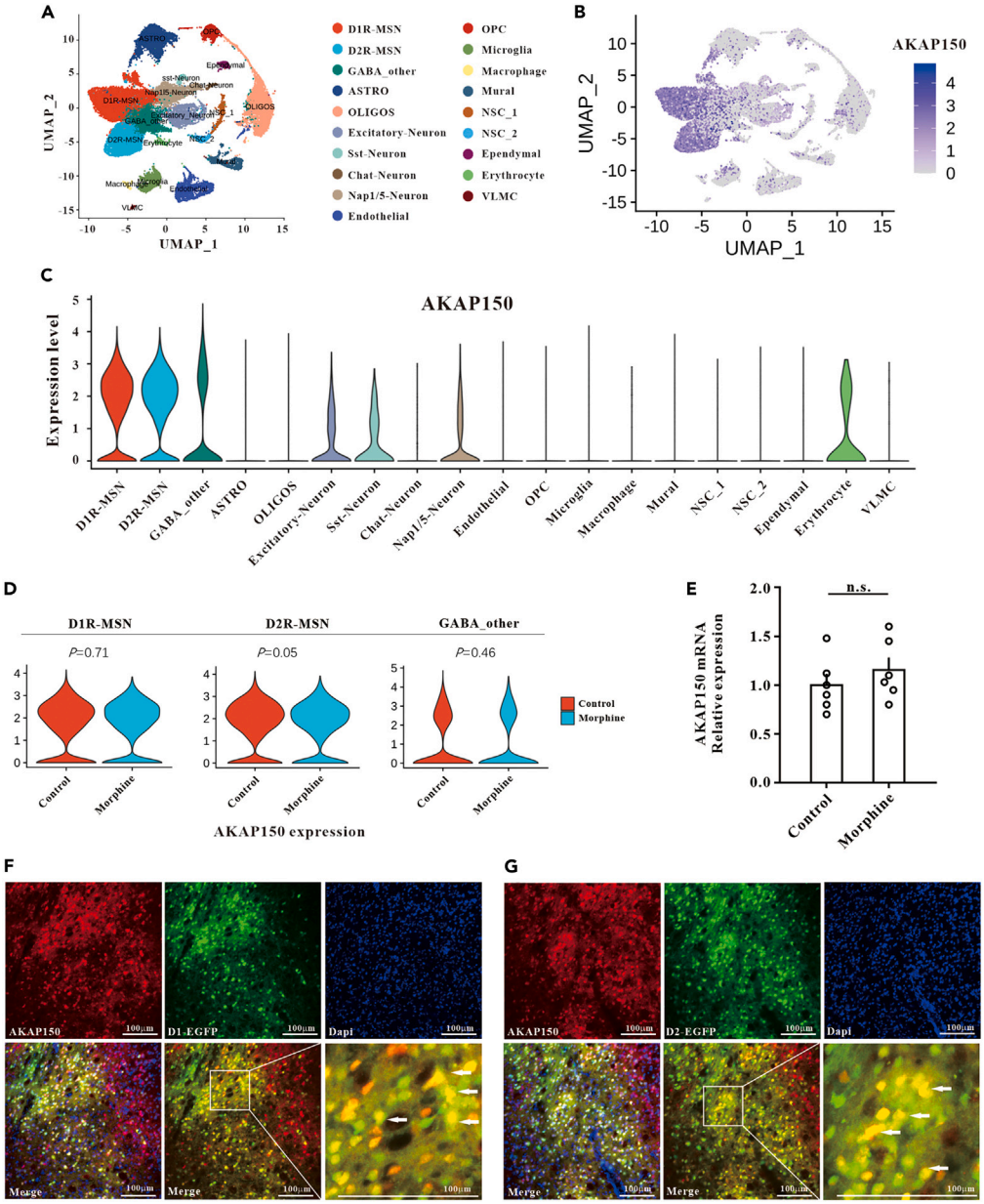

Figure 4. AKAP150 was highly expressed in D1R-MSNs and D2R-MSNs

(A) UMAP plot of 35,878 single cells grouped into 19 major cell types. Each dot represents one single cell, colored according to cell type.

(B) Feature plot of the normalized expression of AKAP150 gene for each cell type and the depth of color from gray to blue represents low to high expression.

(C) Violin plots showed the normalized expression of AKAP150 gene (rows) in each cell cluster (columns). Cell clusters and the expression level of AKAP150 are indicated at the *x* and *y* axis, respectively.

(D) Violin plots showed the normalized expression of AKAP150 gene (rows) from one time morphine-treated mice and saline-treated mice (columns) in D1R-MSN cluster (left), D2R-MSN cluster (middle) and GABA_other cluster (right). Treat group and the expression level of AKAP150 are indicated at the *x* and *y* axis, respectively. p values are derived from two-sided Wilcoxon test.

(E) Level of AKAP150 mRNA relative expression was not significantly changed after one time treatment of morphine compared with saline (N.S. = no significance, $p > 0.05$, t test, $n = 6$).

(F and G) IHC showed expression of AKAP150 in D1 (F) and D2 (G) receptor positive neuron in the naloxone-precipitated morphine withdrawal mice. Scale bar, 100μm. Data are shown as the mean ± SEM.

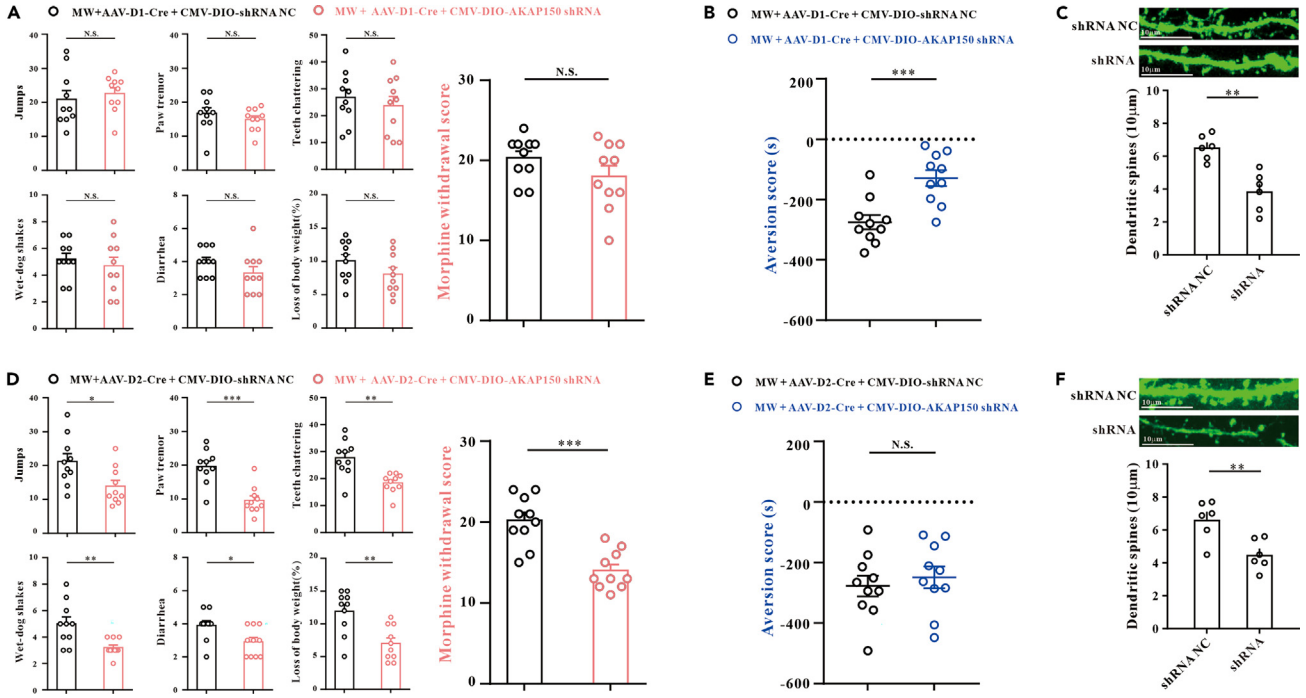

Figure 5. Evaluation of morphine withdrawal score and aversion score after knockdown of AKAP150 in D1R-MSNs or D2R-MSNs in WT mice

(A) Morphine withdrawal somatic signs and morphine withdrawal score showed no significant differences after knockdown of AKAP150 expression in D1R-MSNs in WT mice (N.S. = no significance, $p > 0.05$, t test except diarrhea using Mann-Whitney U test, n = 10).

(B) Aversion score was improved after knockdown of AKAP150 expression in D1R-MSNs in WT mice (***$P<0.001$, t test, n = 10).

(C) Density of dendritic spines was significantly decreased after the knockdown of AKAP150 in D1R-MSNs (**$P<0.01$, t test, n = 6).

(D) Morphine withdrawal somatic signs including jumps (*$P<0.05$, t test, n = 10), paw tremor (***$P<0.001$, t test, n = 10), teeth chattering (**$P<0.01$, t test, n = 10), wet-dog shake (**$P<0.01$, Mann-Whitney U test, n = 10), diarrhea (*$P<0.05$, Mann-Whitney U test, n = 10), and loss of body weight (**$P<0.01$, t test, n = 10) were decreased and morphine withdrawal score (***$P<0.001$, t test, n = 10) was significantly lower after knockdown of AKAP150 expression in D2R-MSNs in WT mice.

(E) Aversion score showed no significant differences after knockdown of AKAP150 expression in D2R-MSNs in WT mice (N.S. = no significance, $p > 0.05$, t test, n = 10).

(F) Density of dendritic spines was significantly decreased after the knockdown of AKAP150 in D2R-MSNs (**$P<0.01$, t test, n = 6). Data are shown as the mean ± SEM.

was not significantly decreased after chronic morphine treatment compared with the control group, which is not consistent with Robinson's study.[34] The impact of the density of dendritic spine in NAc on the process of morphine addiction and withdrawal needs more researches for better clarification.

Distinct functions of AKAP150 in D1R- and D2R-MSNs within the NAc in morphine withdrawal signs

The main output neurons in the NAc are D1R-MSNs and D2R-MSNs. These two main output neurons in the NAc are supposed to exert different functions in the development of morphine withdrawal signs. Firstly, using the single cell RNA-seq, we confirmed that AKAP150 was highly expressed in D1R- and D2R-MSN within the NAc. Previous studies have addressed that D1R- and D2R-MSNs are proposed to play opposing roles in mediating behavioral motivation and reward learning.[3,21] D1R-MSNs are related to persistent reinforcement, whereas D2R-MSNs are related to transient punishment.[21] However, we cannot exclude the possibility that part of MSNs in the NAc expresses both D1 and D2 receptor and play different roles in manipulating neurons of other brain region. In this study, we only explored the effect of MSNs expressing D1R or D2R, meaning that we could not specifically observe the effect of one certain neuron, which would require more investigation in the future.

We selectively suppressed AKAP150 in D1R neurons and D2R neurons, respectively, to find out the effect on the expression of morphine withdrawal induced aversion and somatic signs. To our surprise, the behavioral tests showed that inhibition of AKAP150 in D1R neurons alleviated the conditioned place aversion but did not affect morphine withdrawal somatic signs. Conversely, inhibition of AKAP150 in D2R neurons ameliorated the somatic signs induced by morphine withdrawal without effect on conditioned place aversion. AKAP150 is recognized to bind numerous signaling, substrates, proteins involved in long-term synaptic plasticity.[14] Evidence shows that AKAP150 organizes kinases and phosphatases to regulate AMPA receptors (AMPARs) that are pivotal for synaptic plasticity.[37] Other study illustrates that AKAP150 coordinates PKA and CaN regulation of Ca^{2+}-permeable AMPA-type glutamate receptors to mediate disruption of synaptic plasticity.[38] Chronic drug exposure upregulates cAMP formation, cAMP-dependent PKA activity, and PKA-dependent protein phosphorylation in the NAc.[39] LA Guercio et al.[27] have reported that AKAP150 in the accumbens shell contributes to cocaine reinstatement by facilitating PKA-dependent

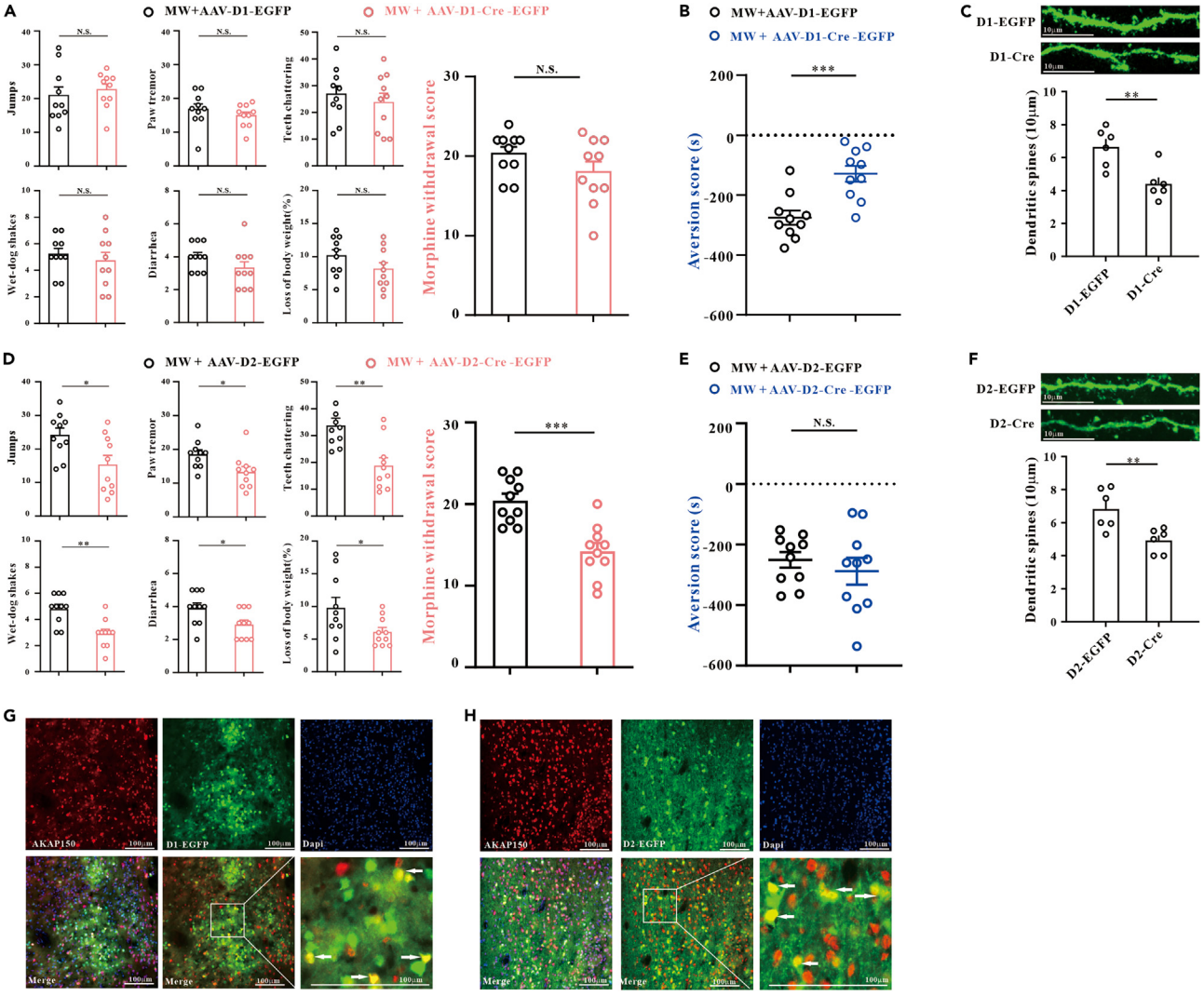

Figure 6. Evaluation of morphine withdrawal score and aversion score after knockdown of AKAP150 in D1R-MSNs or D2R-MSNs in AKAP150 $^{fl/fl}$ mice

(A) Morphine withdrawal somatic signs and morphine withdrawal score showed no significant differences after knockdown of AKAP150 expression in D1R-MSNs in AKAP150 $^{fl/fl}$ mice (N.S. = no significance, $p > 0.05$, t test, n = 10).

(B) Aversion score was improved after knockdown of AKAP150 expression in D1R-MSNs in AKAP150 $^{fl/fl}$ mice (***$P<0.001$, t test, n = 10).

(C) Density of dendritic spines was significantly decreased after the knockdown of AKAP150 in D1R-MSNs (**$P<0.01$, t test, n = 6).

(D) Morphine withdrawal somatic responses including jumps (*$P<0.05$, t test, n = 10), paw tremor (*$P<0.05$, t test, n = 10), teeth chattering (**$P<0.01$, t test, n = 10), wet-dog shake (**$P<0.01$, t test, n = 10), diarrhea (*$P<0.05$, Mann-Whitney U test, n = 10), and loss of body weight (*$P<0.05$, t test, n = 10) were decreased and morphine withdrawal score (***$P<0.001$, t test, n = 10) was significantly lower after knockdown of AKAP150 expression in D2R-MSNs in AKAP150 $^{fl/fl}$ mice.

(E) Aversion score showed no significant differences after knockdown of AKAP150 expression in D2R-MSNs in AKAP150 $^{fl/fl}$ mice (N.S. = no significance, $p > 0.05$, t test, n = 10).

(F) Density of dendritic spines was significantly decreased after the knockdown of AKAP150 in D2R-MSNs (**$P<0.01$, t test, n = 6).

(G) IHC demonstrated double labeling of AKAP150 and D1-MSNs in the AKAP150 $^{fl/fl}$ mice.

(H) IHC demonstrated double labeling of AKAP150 and D1-MSNs in the AKAP150 $^{fl/fl}$ mice. Scale bar, 100μm. Data are shown as the mean ± SEM.

phosphorylation of GluA1-containing AMPRs, suggesting that AKAP150 is necessary to bridge the dopamine and glutamate systems in the NAc during drug seeking. Furthermore, AKAP150 signaling complex has been proven to regulate the sensitization of transient receptor potential type V1 (TRPV1) in peripheral nociception.[40]

Integrally, AKAP150 is an attractive candidate target for neuropsychiatric disorder which exerts vast functions via different signaling pathway. In our present study, we did not explore the underlying mechanism how AKAP150 within the NAc regulates the morphine withdrawal signs, thus more in-depth research will be required.

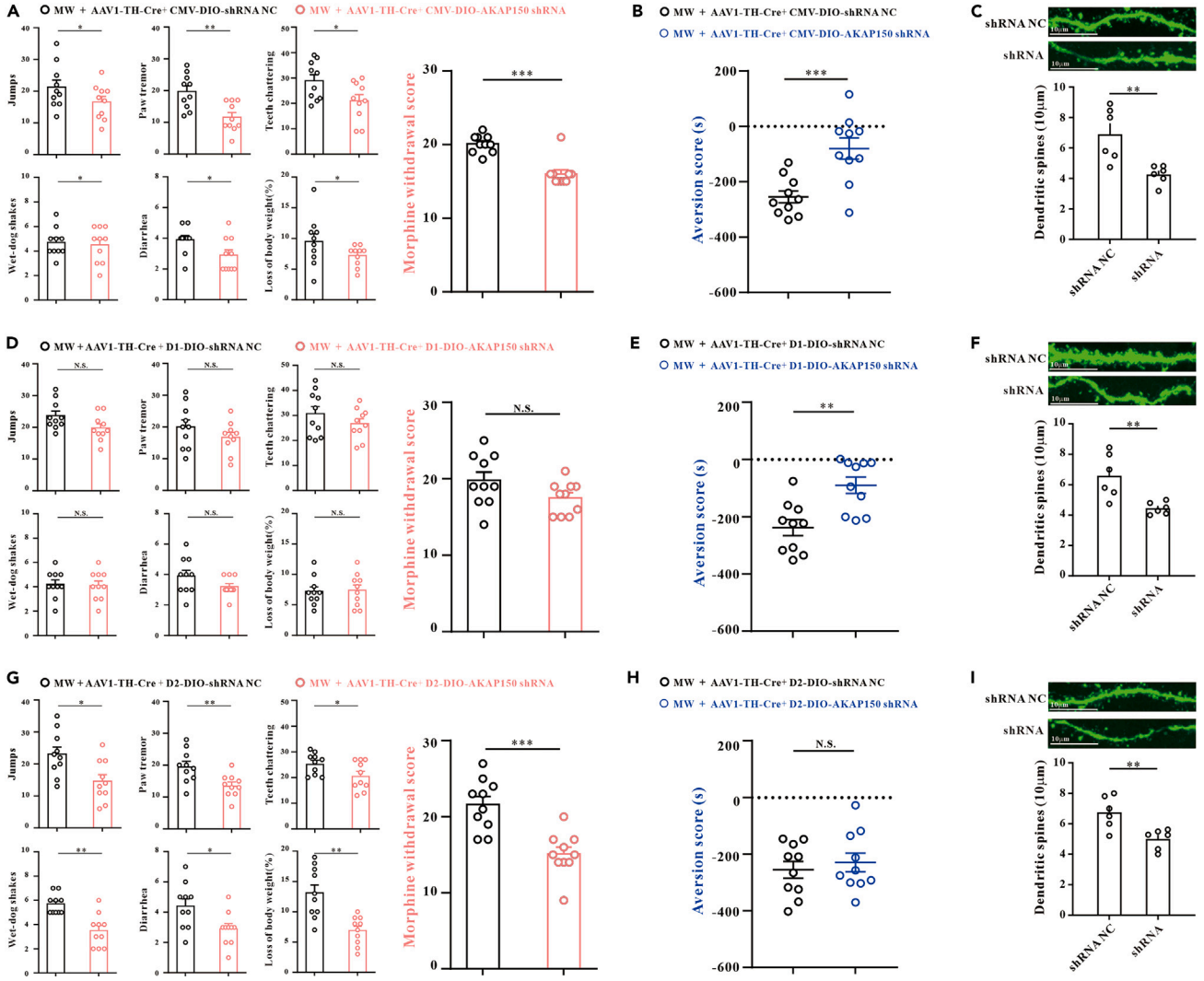

Figure 7. Activity of AKAP150 expressed in D1R-MSNs and D2R-MSNs in NAc received mediation from VTA

(A and B) AAV1-TH-Cre in VTA promoted the expression of CMV-DIO-shRNA-EGFP in NAc and relieved the morphine withdrawal somatic signs including jumps (*P<0.05, t test, n = 10), paw tremor (**P<0.01, t test, n = 10), teeth chattering (*P<0.05, t test, n = 10), wet-dog shake (*P<0.05, t test, n = 10), diarrhea (*P<0.05, Mann-Whitney U test, n = 10), and loss of body weight (*P<0.05, t test, n = 10), and morphine withdrawal score (***P<0.001, t test, n = 10) was significantly lower (A) as well as the CPA scores (***P<0.001, t test, n = 10) (B).

(C) Density of dendritic spines was significantly decreased after the knockdown of AKAP150 in the NAc mediated by VTA (**P<0.01, t test, n = 6).

(D and E) Inhibition of AKAP150 in D1R-MSNs receiving projections from VTA relieved the morphine withdrawal aversion (**P<0.01, t test, n = 10) (E) without relieving morphine withdrawal somatic signs (N.S. = no significance, $p > 0.05$, t test except diarrhea using Mann-Whitney U test, n = 10) (D).

(F) Density of dendritic spines was significantly decreased after inhibition of AKAP150 in D1R-MSNs receiving projections from VTA (**P<0.01, t test, n = 6).

(G and H) Inhibition of AKAP150 in D2R-MSNs receiving projections from VTA relieved the morphine withdrawal somatic signs [jumps (*P<0.05, t test, n = 10), paw tremor (**P<0.01, t test, n = 10), teeth chattering (*P<0.05, t test, n = 10), wet-dog shake (**P<0.01, Mann-Whitney U test, n = 10), diarrhea (*P<0.05, t test, n = 10), loss of body weight (**P<0.01, t test, n = 10), and morphine withdrawal score (***P<0.001, t test, n = 10)] (G) without relieving the morphine withdrawal aversion (N.S. = no significance, $p > 0.05$, t test, n = 10) (H).

(I) Density of dendritic spines was significantly decreased after inhibition of AKAP150 in D2R-MSNs receiving projections from VTA (**P<0.01, t test, n = 6). Data are shown as the mean ± SEM.

Manipulating the AKAP150 in D1R- and D2R-MSNs from VTA→NAc modulated morphine withdrawal signs

Dopamine neurons in the VTA and their projections to the NAc and other limbic regions in the forebrain comprise the mesolimbic system, which plays an important role in mediating drug reward and withdrawal in drug abuse. As the rate-limiting enzyme in dopamine biosynthesis, an upregulation of TH expression increases the synthesis of dopamine.[41]

Evidence indicates that the mesostriatal dopamine system consists projections from the VTA to the ventral striatum mainly the NAc, which is considered to code the salience and valence not only of rewarding but also aversive stimuli.[42] Besides, the projections from VTA→NAc display heterogeneous intrinsic properties and play key roles in the pain-related affective behaviors, stress-induced depression, as well as nociceptive modulation.[43–45] However, whether and how the inputs/projections from the VTA→NAc regulate morphine withdrawal signs related to AKAP150 expressed in D1R- and D2R MSNs is still unknown. Evidence shows that AAV1 can be transported anterogradely and can transsynaptically transduce neuronal populations in brain regions postsynaptic to a given injection site.[46] As a small number of AAV1 particles are transported transneuronally from the initial host cell, utilizing Cre as an amplification step can unlock robust transgene expression. When combined with a conditional expression strategy, this transsynaptic transport property enables us to reveal the relationship between the level of TH in VTA and the expression of AKAP150 in NAc. In our present study, we injected AAV1-TH-EGFP as a tracer into the VTA, and then we found that the injection of AAV1-TH-Cre into VTA promoted the expression of CMV-DIO-shRNA-EGFP in the NAc and relieved the morphine withdrawal somatic signs and CPA scores. This result illustrates that the projections from the VTA to the NAc may involve in the development of morphine withdrawal induced aversion and somatic signs. Then we further specifically inhibited AKAP150 expressed in the D1R-MSNs or D2R-MSNs which received projections from the VTA. Interestingly, we found that specifically inhibition of AKAP150 in the D1R-MSNs which received projections from the VTA could relieve the morphine withdrawal aversion, but could not relieve the morphine withdrawal induced somatic signs. Conversely, the inhibition of AKAP150 in the D2R- MSNs which received projections from the VTA could relieve the somatic signs but not the aversion. In Zhu's study,[3] depotentiation of the paraventricular nucleus of the thalamus (PVT)→D2-MSN synapses reduced the immediate expression of withdrawal behavioral symptoms and the aversive memory of the withdrawal chamber, while such effects were not observed at the PVT→D1-MSN synapses. Though the role of D2-MSN or D1-MSN in Zhu's study is not completely consistent with our study, inhibition of D2-MSN in NAc alleviated the morphine withdrawal somatic signs in both studies. We think the discrepancy is mainly because the neuronal circuits investigated in the two studies are not the same. And neurons in the same region receiving projection from different areas of the brain might exert different or even opposing effects. We assume that the projections from VTA to D1R- and D2R-MSNs within the NAc play a key role in the regulation of morphine withdrawal signs, and AKAP150 exerts prominent functions in this process. However, Jalali et al.[47] reported that neither chronic morphine treatment nor morphine withdrawal induces significant alterations in the TH mRNA expression in the VTA. In our study, we did not conduct tests to confirm the changes of TH level after prolonged morphine treatment and morphine withdrawal. To further elucidate the underlying mechanism, we should investigate experiments to evaluate the changes in TH mRNA and TH expression during chronic morphine treatment and morphine withdrawal.

In conclusion, upregulation of AKAP150 expression in the NAc is relevant with the development of morphine induced aversion and somatic signs via suppressing neurons activities and regulating the plasticity of the dendritic spines of MSNs. Inhibition of AKAP150 from NAc D1R-MSNs relieves morphine withdrawal aversion, and inhibition of AKAP150 from NAc D2R-MSNs alleviates morphine withdrawal somatic responses, which may be a drug development target for the treatment of addiction and relapse. Further studies are required to explain how AKAP150 is modulated by upstream signaling.

Limitations of the study

The present study demonstrated that AKAP150 from D1R-MSNs or D2R-MSNs in NAc contributed to the developmental process of morphine withdrawal but played different roles in modulation of morphine withdrawal somatic signs and aversive memory. However, the underlying mechanism of how AKAP150 within the NAc D1R-MSNs or D2R-MSNs regulates the morphine withdrawal signs and aversive memory needs more in-depth researches to be clarified. And experiments about the changes in TH mRNA and TH expression in VTA during chronic morphine treatment and morphine withdrawal are not included in this study.

STAR★METHODS

Detailed methods are provided in the online version of this paper and include the following:

- KEY RESOURCES TABLE
- RESOURCE AVAILABILITY
  - Lead contact
  - Materials availability
  - Data and code availability
- EXPERIMENTAL MODEL AND STUDY PARTICIPANT DETAILS
  - Animals
- METHOD DETAILS
  - Evaluation of naloxone-precipitated morphine withdrawal somatic signs
  - Morphine withdrawal Conditioned Place Aversion (CPA)
  - Surgeries and stereotaxic injections
  - AKAP150 knockdown
  - Immunohistochemical (IHC) analyses
  - Western blotting

- RNA extraction and real-time quantitative polymerase chain reaction (PCR)
- Dendritic spine analysis
- Bioinformatic analysis of ScRNA-seq data

- QUANTIFICATION AND STATISTICAL ANALYSIS

SUPPLEMENTAL INFORMATION

Supplemental information can be found online at https://doi.org/10.1016/j.isci.2023.108227.

ACKNOWLEDGMENTS

This work was supported by the National Natural Science Foundation of China (82071237 and 81771192), and Guangdong Basic and Applied Basic Research Foundation (2023A1515010147 and 2023A1515011180).

AUTHOR CONTRIBUTIONS

H.D.O.Y., K.Z., X.H.B., and J.X.Z. designed the experiment. C.P.O. and H.D.O.Y. wrote the manuscript. K.Z., Y.J.Z., D.M.C., Y.Y.M., X.L.L., and W.H. performed experiments and collected the data. Y.Y.M., X.H.B., H.D.O.Y., and K.Z. performed analysis. W.H. and H.D.O.Y. supervised this study.

DECLARATION OF INTERESTS

The authors declare no competing interests.

Received: June 14, 2023
Revised: August 22, 2023
Accepted: October 13, 2023
Published: October 17, 2023

REFERENCES

1. Waldhoer, M., Bartlett, S.E., and Whistler, J.L. (2004). Opioid Receptors. Annu. Rev. Biochem. *73*, 953–990. https://doi.org/10.1146/annurev.biochem.73.011303.073940.
2. Volkow, N.D., Jones, E.B., Einstein, E.B., and Wargo, E.M. (2019). Prevention and Treatment of Opioid Misuse and Addiction. JAMA Psychiatr. *76*, 208–216. https://doi.org/10.1001/jamapsychiatry.2018.3126.
3. Zhu, Y., Wienecke, C.F.R., Nachtrab, G., and Chen, X. (2016). A thalamic input to the nucleus accumbens mediates opiate dependence. Nature *530*, 219–222. https://doi.org/10.1038/nature16954.
4. Herscher, M., Fine, M., Navalurkar, R., Hirt, L., and Wang, L. (2020). Diagnosis and Management of Opioid Use Disorder in Hospitalized Patients. Med. Clin. North Am. *104*, 695–708. https://doi.org/10.1016/j.mcna.2020.03.003.
5. Srivastava, A.B., Mariani, J.J., and Levin, F.R. (2020). New directions in the treatment of opioid withdrawal. Lancet *395*, 1938–1948. https://doi.org/10.1016/s0140-6736(20)30852-7.
6. Navarro-Zaragoza, J., Hidalgo, J.M., Laorden, M.L., and Milanés, M.V. (2012). Glucocorticoid receptors participate in the opiate withdrawal-induced stimulation of rats NTS noradrenergic activity and in the somatic signs of morphine withdrawal. Br. J. Pharmacol. *166*, 2136–2147. https://doi.org/10.1111/j.1476-5381.2012.01918.x.
7. McGregor, R., Wu, M.F., Holmes, B., Lam, H.A., Maidment, N.T., Gera, J., Yamanaka, A., and Siegel, J.M. (2022). Hypocretin/Orexin Interactions with Norepinephrine Contribute to the Opiate Withdrawal Syndrome. J. Neurosci. *42*, 255–263. https://doi.org/10.1523/JNEUROSCI.1557-21.2021.
8. Kreek, M.J., Levran, O., Reed, B., Schlussman, S.D., Zhou, Y., and Butelman, E.R. (2012). Opiate addiction and cocaine addiction: underlying molecular neurobiology and genetics. J. Clin. Invest. *122*, 3387–3393. https://doi.org/10.1172/jci60390.
9. Hyman, S.E., Malenka, R.C., and Nestler, E.J. (2006). NEURAL MECHANISMS OF ADDICTION: The Role of Reward-Related Learning and Memory. Annu. Rev. Neurosci. *29*, 565–598. https://doi.org/10.1146/annurev.neuro.29.051605.113009.
10. Browne, C.J., Godino, A., Salery, M., and Nestler, E.J. (2020). Epigenetic Mechanisms of Opioid Addiction. Biol. Psychiatry *87*, 22–33. https://doi.org/10.1016/j.biopsych.2019.06.027.
11. Salgado, S., and Kaplitt, M.G. (2015). The Nucleus Accumbens: A Comprehensive Review. Stereotact. Funct. Neurosurg. *93*, 75–93. https://doi.org/10.1159/000368279.
12. Sheng, H., Lei, C., Yuan, Y., Fu, Y., Cui, D., Yang, L., Shao, D., Cao, Z., Yang, H., Guo, X., et al. (2023). Nucleus accumbens circuit disinhibits lateral hypothalamus glutamatergic neurons contributing to morphine withdrawal memory in male mice. Nat. Commun. *14*, 71. https://doi.org/10.1038/s41467-022-35758-5.
13. Nie, B., Liu, C., Bai, X., Chen, X., Wu, S., Zhang, S., Huang, Z., Xie, M., Xu, T., Xin, W., et al. (2018). AKAP150 involved in paclitaxel-induced neuropathic pain via inhibiting CN/NFAT2 pathway and downregulating IL-4. Brain Behav. Immun. *68*, 158–168. https://doi.org/10.1016/j.bbi.2017.10.015.
14. Sanderson, J.L., and Dell'Acqua, M.L. (2011). AKAP Signaling Complexes in Regulation of Excitatory Synaptic Plasticity. Neuroscientist *17*, 321–336. https://doi.org/10.1177/1073858410384740.
15. Reissner, K.J., Uys, J.D., Schwacke, J.H., Comte-Walters, S., Rutherford-Bethard, J.L., Dunn, T.E., Blumer, J.B., Schey, K.L., and Kalivas, P.W. (2011). AKAP Signaling in Reinstated Cocaine Seeking Revealed by iTRAQ Proteomic Analysis. J. Neurosci. *31*, 5648–5658. https://doi.org/10.1523/jneurosci.3452-10.2011.
16. Lammel, S., Ion, D.I., Roeper, J., and Malenka, R.C. (2011). Projection-Specific Modulation of Dopamine Neuron Synapses by Aversive and Rewarding Stimuli. Neuron *70*, 855–862. https://doi.org/10.1016/j.neuron.2011.03.025.
17. Yuen, J., Goyal, A., Rusheen, A.E., Kouzani, A.Z., Berk, M., Kim, J.H., Tye, S.J., Blaha, C.D., Bennet, K.E., Lee, K.H., et al. (2023). High frequency deep brain stimulation can mitigate the acute effects of cocaine administration on tonic dopamine levels in the rat nucleus accumbens. Front. Neurosci. *17*, 1061578. https://doi.org/10.3389/fnins.2023.1061578.
18. Soares-Cunha, C., de Vasconcelos, N.A.P., Coimbra, B., Domingues, A.V., Silva, J.M., Loureiro-Campos, E., Gaspar, R., Sotiropoulos, I., Sousa, N., and Rodrigues, A.J. (2020). Nucleus accumbens medium spiny neurons subtypes signal both reward and aversion. Mol. Psychiatry *25*, 3241–3255. https://doi.org/10.1038/s41380-019-0484-3.
19. Lin, Y.-H., Yamahashi, Y., Kuroda, K., Faruk, M.O., Zhang, X., Yamada, K., Yamanaka, A., Nagai, T., and Kaibuchi, K. (2021). Accumbal D2R-medium spiny neurons regulate aversive behaviors through PKA-Rap1 pathway. Neurochem. Int. *143*, 104935. https://doi.org/10.1016/j.neuint.2020.104935.

20. Lobo, M.K., Covington, H.E., Chaudhury, D., Friedman, A.K., Sun, H., Damez-Werno, D., Dietz, D.M., Zaman, S., Koo, J.W., Kennedy, P.J., et al. (2010). Cell Type–Specific Loss of BDNF Signaling Mimics Optogenetic Control of Cocaine Reward. Science *330*, 385–390. https://doi.org/10.1126/science.1188472.
21. Kravitz, A.V., Tye, L.D., and Kreitzer, A.C. (2012). Distinct roles for direct and indirect pathway striatal neurons in reinforcement. Nat. Neurosci. *15*, 816–818. https://doi.org/10.1038/nn.3100.
22. Soares-Cunha, C., Coimbra, B., David-Pereira, A., Borges, S., Pinto, L., Costa, P., Sousa, N., and Rodrigues, A.J. (2016). Activation of D2 dopamine receptor-expressing neurons in the nucleus accumbens increases motivation. Nat. Commun. *7*, 11829. https://doi.org/10.1038/ncomms11829.
23. Björklund, A., and Dunnett, S.B. (2007). Dopamine neuron systems in the brain: an update. Trends Neurosci. *30*, 194–202. https://doi.org/10.1016/j.tins.2007.03.006.
24. Avey, D., Sankararaman, S., Yim, A.K.Y., Barve, R., Milbrandt, J., and Mitra, R.D. (2018). Single-Cell RNA-Seq Uncovers a Robust Transcriptional Response to Morphine by Glia. Cell Rep. *24*, 3619–3629.e4. https://doi.org/10.1016/j.celrep.2018.08.080.
25. Shepard, R.D., Langlois, L.D., Authement, M.E., and Nugent, F.S. (2020). Histone deacetylase inhibition reduces ventral tegmental area dopamine neuronal hyperexcitability involving AKAP150 signaling following maternal deprivation in juvenile male rats. J. Neurosci. Res. *98*, 1457–1467. https://doi.org/10.1002/jnr.24613.
26. Purkey, A.M., Woolfrey, K.M., Crosby, K.C., Stich, D.G., Chick, W.S., Aoto, J., and Dell'Acqua, M.L. (2018). AKAP150 Palmitoylation Regulates Synaptic Incorporation of Ca2+-Permeable AMPA Receptors to Control LTP. Cell Rep. *25*, 974–987.e4. https://doi.org/10.1016/j.celrep.2018.09.085.
27. Guercio, L.A., Hofmann, M.E., Swinford-Jackson, S.E., Sigman, J.S., Wimmer, M.E., Dell'Acqua, M.L., Schmidt, H.D., and Pierce, R.C. (2018). A-Kinase Anchoring Protein 150 (AKAP150) Promotes Cocaine Reinstatement by Increasing AMPA Receptor Transmission in the Accumbens Shell. Neuropsychopharmacology *43*, 1395–1404. https://doi.org/10.1038/npp.2017.297.
28. Georges, F., Stinus, L., and Le Moine, C. (2000). Mapping ofc-fosgene expression in the brain during morphine dependence and precipitated withdrawal, and phenotypic identification of the striatal neurons involved. Eur. J. Neurosci. *12*, 4475–4486. https://doi.org/10.1046/j.0953-816X.2000.01334.x.
29. Thompson, B.L., Oscar-Berman, M., and Kaplan, G.B. (2021). Opioid-induced structural and functional plasticity of medium-spiny neurons in the nucleus accumbens. Neurosci. Biobehav. Rev. *120*, 417–430. https://doi.org/10.1016/j.neubiorev.2020.10.015.
30. Geoffroy, H., Canestrelli, C., Marie, N., and Noble, F. (2019). Morphine-Induced Dendritic Spine Remodeling in Rat Nucleus Accumbens Is Corticosterone Dependent. Int. J. Neuropsychopharmacol. *22*, 394–401. https://doi.org/10.1093/ijnp/pyz014.
31. Bowers, M.S., Chen, B.T., and Bonci, A. (2010). AMPA Receptor Synaptic Plasticity Induced by Psychostimulants: The Past, Present, and Therapeutic Future. Neuron *67*, 11–24. https://doi.org/10.1016/j.neuron.2010.06.004.
32. Maze, I., Covington, H.E., Dietz, D.M., LaPlant, Q., Renthal, W., Russo, S.J., Mechanic, M., Mouzon, E., Neve, R.L., Haggarty, S.J., et al. (2010). Essential Role of the Histone Methyltransferase G9a in Cocaine-Induced Plasticity. Science *327*, 213–216. https://doi.org/10.1126/science.1179438.
33. Russo, S.J., Dietz, D.M., Dumitriu, D., Morrison, J.H., Malenka, R.C., and Nestler, E.J. (2010). The addicted synapse: mechanisms of synaptic and structural plasticity in nucleus accumbens. Trends Neurosci. *33*, 267–276. https://doi.org/10.1016/j.tins.2010.02.002.
34. Robinson, T.E., Gorny, G., Savage, V.R., and Kolb, B. (2002). Widespread but regionally specific effects of experimenter- versus self-administered morphine on dendritic spines in the nucleus accumbens, hippocampus, and neocortex of adult rats. Synapse *46*, 271–279. https://doi.org/10.1002/syn.10146.
35. Diana, M., Spiga, S., and Acquas, E. (2006). Persistent and Reversible Morphine Withdrawal-Induced Morphological Changes in the Nucleus Accumbens. Ann. N. Y. Acad. Sci. *1074*, 446–457. https://doi.org/10.1196/annals.1369.045.
36. Kasture, S., Vinci, S., Ibba, F., Puddu, A., Marongiu, M., Murali, B., Pisanu, A., Lecca, D., Zernig, G., and Acquas, E. (2009). Withania somnifera Prevents Morphine Withdrawal-Induced Decrease in Spine Density in Nucleus Accumbens Shell of Rats: A Confocal Laser Scanning Microscopy Study. Neurotox. Res. *16*, 343–355. https://doi.org/10.1007/s12640-009-9069-2.
37. Li, Y., Bai, X., Gao, M., Chen, H., Ma, X., Zhang, Y., Bai, H., Liu, Y., Hu, X., and Suo, Z. (2021). AKAP150 and its Palmitoylation Contributed to Pain Hypersensitivity Via Facilitating Synaptic Incorporation of GluA1-Containing AMPA Receptor in Spinal Dorsal Horn. Mol. Neurobiol. *58*, 6505–6519. https://doi.org/10.1007/s12035-021-02570-z.
38. Sanderson, J.L., Freund, R.K., Gorski, J.A., and Dell'Acqua, M.L. (2021). β-Amyloid disruption of LTP/LTD balance is mediated by AKAP150-anchored PKA and Calcineurin regulation of Ca2+-permeable AMPA receptors. Cell Rep. *37*, 109786. https://doi.org/10.1016/j.celrep.2021.109786.
39. Self, D.W., Genova, L.M., Hope, B.T., Barnhart, W.J., Spencer, J.J., and Nestler, E.J. (1998). Involvement of cAMP-Dependent Protein Kinase in the Nucleus Accumbens in Cocaine Self-Administration and Relapse of Cocaine-Seeking Behavior. J. Neurosci. *18*, 1848–1859. https://doi.org/10.1523/jneurosci.18-05-01848.1998.
40. Jeske, N.A., Diogenes, A., Ruparel, N.B., Fehrenbacher, J.C., Henry, M., Akopian, A.N., and Hargreaves, K.M. (2008). A-kinase anchoring protein mediates TRPV1 thermal hyperalgesia through PKA phosphorylation of TRPV1. Pain *138*, 604–616. https://doi.org/10.1016/j.pain.2008.02.022.
41. Grasing, K., Bills, D., Ghosh, S., Schlussman, S.D., Patel, A.H., and Woodward, J.J. (1997). Opiate modulation of striatal dopamine and hippocampal norepinephrine release following morphine withdrawal. Neurochem. Res. *22*, 239–248. https://doi.org/10.1023/a:1022474318541.
42. Lammel, S., Lim, B.K., and Malenka, R.C. (2014). Reward and aversion in a heterogeneous midbrain dopamine system. Neuropharmacology *76*, 351–359. https://doi.org/10.1016/j.neuropharm.2013.03.019.
43. Liu, D., Tang, Q.-Q., Yin, C., Song, Y., Liu, Y., Yang, J.-X., Liu, H., Zhang, Y.-M., Wu, S.-Y., Song, Y., et al. (2018). Brain-derived neurotrophic factor–mediated projection-specific regulation of depressive-like and nociceptive behaviors in the mesolimbic reward circuitry. Pain *159*, 175. https://doi.org/10.1097/j.pain.0000000000001083.
44. Deisseroth, K. (2014). Circuit dynamics of adaptive and maladaptive behaviour. Nature *505*, 309–317. https://doi.org/10.1038/nature12982.
45. Schwartz, N., Temkin, P., Jurado, S., Lim, B.K., Heifets, B.D., Polepalli, J.S., and Malenka, R.C. (2014). Decreased motivation during chronic pain requires long-term depression in the nucleus accumbens. Science *345*, 535–542. https://doi.org/10.1126/science.1253994.
46. Zingg, B., Chou, X.-L., Zhang, Z.-G., Mesik, L., Liang, F., Tao, H.W., and Zhang, L.I. (2017). AAV-Mediated Anterograde Transsynaptic Tagging: Mapping Corticocollicular Input-Defined Neural Pathways for Defense Behaviors. Neuron *93*, 33–47. https://doi.org/10.1016/j.neuron.2016.11.045.
47. Jalali Mashayekhi, F., Rasti, M., Khoshdel, Z., and Owji, A.A. (2018). Expression Levels of the Tyrosine Hydroxylase Gene and Histone Modifications Around its Promoter in the Locus Coeruleus and Ventral Tegmental Area of Rats during Forced Abstinence from Morphine. Eur. Addict. Res. *24*, 304–311. https://doi.org/10.1159/000495362.
48. Stuart, T., Butler, A., Hoffman, P., Hafemeister, C., Papalexi, E., Mauck, W.M., Hao, Y., Stoeckius, M., Smibert, P., and Satija, R. (2019). Comprehensive Integration of Single-Cell Data. Cell *177*, 1888–1902.e21. https://doi.org/10.1016/j.cell.2019.05.031.
49. McGinnis, C.S., Murrow, L.M., and Gartner, Z.J. (2019). DoubletFinder: Doublet Detection in Single-Cell RNA Sequencing Data Using Artificial Nearest Neighbors. Cell Syst. *8*, 329–337.e4. https://doi.org/10.1016/j.cels.2019.03.003.
50. Korsunsky, I., Millard, N., Fan, J., Slowikowski, K., Zhang, F., Wei, K., Baglaenko, Y., Brenner, M., Loh, P.-R., and Raychaudhuri, S. (2019). Fast, sensitive and accurate integration of single-cell data with Harmony. Nat. Methods *16*, 1289–1296. https://doi.org/10.1038/s41592-019-0619-0.
51. Bai, X., Zhang, K., Ou, C., Nie, B., Zhang, J., Huang, Y., Zhang, Y., Huang, J., Ouyang, H., Cao, M., and Huang, W. (2023). Selective activation of AKAP150/TRPV1 in ventrolateral periaqueductal gray GABAergic neurons facilitates conditioned place aversion in male mice. Commun. Biol. *6*, 742. https://doi.org/10.1038/s42003-023-05106-4.
52. Zhang, L., Kibaly, C., Wang, Y.J., Xu, C., Song, K.Y., McGarrah, P.W., Loh, H.H., Liu, J.G., and Law, P.Y. (2017). Src-dependent phosphorylation of μ-opioid receptor at Tyr336 modulates opiate withdrawal. EMBO Mol. Med. *9*, 1521–1536. https://doi.org/10.15252/emmm.201607324.
53. Maldonado, R., Blendy, J.A., Tzavara, E., Gass, P., Roques, B.P., Hanoune, J., and Schütz, G. (1996). Reduction of morphine

abstinence in mice with a mutation in the gene encoding CREB. Science *273*, 657–659. https://doi.org/10.1126/science.273.5275.657.

54. Zachariou, V., Brunzell, D.H., Hawes, J., Stedman, D.R., Bartfai, T., Steiner, R.A., Wynick, D., Langel, U., and Picciotto, M.R. (2003). The neuropeptide galanin modulates behavioral and neurochemical signs of opiate withdrawal. Proc. Natl. Acad. Sci. USA *100*, 9028–9033. https://doi.org/10.1073/pnas.1533224100.

55. Papaleo, F., and Contarino, A. (2006). Gender- and morphine dose-linked expression of spontaneous somatic opiate withdrawal in mice. Behav. Brain Res. *170*, 110–118. https://doi.org/10.1016/j.bbr.2006.02.009.

56. Cruz, H.G., Berton, F., Sollini, M., Blanchet, C., Pravetoni, M., Wickman, K., and Lüscher, C. (2008). Absence and Rescue of Morphine Withdrawal in GIRK-Kir3 Knock-out Mice. J. Neurosci. *28*, 4069–4077. https://doi.org/10.1523/JNEUROSCI.0267-08.2008.

STAR★METHODS

KEY RESOURCES TABLE

REAGENT or RESOURCE	SOURCE	IDENTIFIER
Antibodies		
Mouse monoclonal anti-AKAP150	Santa Cruz	Cat# sc-377055; RRID: AB_3073565
Rabbit monoclonal anti-c-fos	Abcam	Cat# ab222699; RRID: AB_2891049
Mouse monoclonal anti-TH	Merck	Cat# MAB318; RRID: AB_2201528
Mouse monoclonal anti-β-actin	Proteintech	Cat# 66009-1; RRID: AB_2687938
Bacterial and virus strains		
rAAV-CMV-AKAP150-shRNA-mCherry	Brain VTA	N/A
rAAV-CMV- shRNA-NC-mCherry	Brain VTA	N/A
rAAV-CMV-Cre-EGFP	Brain VTA	Cat# PT-0253
rAAV-CMV-EGFP	Brain VTA	Cat# PT-0693
rAAV-CMV-DIO-AKAP150-shRNA-mCherry	Brain VTA	N/A
rAAV-CMV-DIO-shRNA-NC-mCherry	Brain VTA	N/A
rAAV-D1-Cre-EGFP	Brain VTA	Cat# PT-0812
rAAV-D2-Cre-EGFP	Brain VTA	Cat# PT-0813
rAAV-D1-EGFP	Brain VTA	Cat# PT-0214
rAAV-D2-EGFP	Brain VTA	Cat# PT-3245
rAAV-D1-DIO-AKAP150-shRNA-mCherry	Brain VTA	N/A
rAAV-D1-DIO-shRNA-NC-mCherry	Brain VTA	N/A
rAAV-D2-DIO-AKAP150-shRNA-mCherry	Brain VTA	N/A
rAAV-D2-DIO-shRNA-NC-mCherry	Brain VTA	N/A
AAV1-TH-Cre-EGFP	Brain VTA	Cat# PT-0179
rAAV-D1-mCherry	Brain VTA	Cat# PT-0757
rAAV-D2-mCherry	Brain VTA	Cat# PT-0367
Hysn-FLP: FDIO-EGFP	Brain Case	Cat# BC-SL021
Critical commercial assays		
Evo M-MLV RT Premix for qPCR	Accurate Biotechnology	Cat# AG111706
Experimental models: Organisms/strains		
C57/BL6 mice	Institute of Guangdong Medicine Experimental Animal Center	N/A
AKAP150$^{fl/fl}$ mice	Jackson Laboratory	N/A
Deposited data		
scRNA-seq data of GBM samples	Avey et al.[24]	GEO: GSE118918
Oligonucleotides		
Primer: AKAP150 Forward: 5′-AGGATGGGGCTCTTCCTAAG-3′	This paper	N/A
Software and algorithms		
JLBehv-CPPM-4	Jiliang Technology Co.	N/A
Microsoft Excel	Microsoft	RRID:SCR_016137
ImageJ	NIH	https://imagej.net/
Seurat	Stuart et al.[48]	https://cell.com/cell/fulltext/S0092-8674(19)30559-8

(*Continued on next page*)

Continued

REAGENT or RESOURCE	SOURCE	IDENTIFIER
"DoubletFinder" algorithm	Zev et al.[49]	https://cell.com/cell-systems/fulltext/S2405-4712(19)30073-0
Harmony algorithm	Korsunsky et al.[50]	https://nature.com/articles/s41592-019-0619-0
SPSS	IBM	RRID:SCR_002865

RESOURCE AVAILABILITY

Lead contact

Further information and requests for resources and reagents should be directed to and will be fulfilled by the lead contact, Handong Ouyang (ouyhd@sysucc.org.cn).

Materials availability

This study did not generate new unique reagents.

Data and code availability

- This paper analyzes existing, publicly available data. The accession number for the dataset is listed in the key resources table. All data reported in this paper will be shared by the lead contact upon request.
- This paper does not report original code.
- Any additional information required to reanalyze the data reported in this paper is available from the lead contact upon request.

EXPERIMENTAL MODEL AND STUDY PARTICIPANT DETAILS

Animals

Male C57/BL6 mice (8-10 weeks old) were obtained from the Institute of Guangdong Medicine Experimental Animal Center. AKAP150$^{flox/flox}$ (AKAP150$^{fl/fl}$) mice, which had been used in previous research,[13,51] were purchased from the Jackson Laboratory. All mice were housed at a temperature of 25 ± 1°C and a humidity of 50% to 60%, with free access to food and water. All experimental procedures were approved by the Institutional Animal Care and Use Committee of Sun Yat-sen University. The researchers were blinded to the animal behavior tests after drug treatment.

METHOD DETAILS

Evaluation of naloxone-precipitated morphine withdrawal somatic signs

The naloxone-precipitated morphine withdrawal test was conducted as follows. The test consisted of two pre-test days, four consecutive drug treatment days, and one test day. On Day 1 and 2, each mouse was placed in a transparent box and observed for involuntary movements such as jumps, paw tremors, teeth chattering, wet dog shakes, or diarrhea without any artificial disturbance. Mice that exhibited such movements were excluded from the test. On the following four days, all mice were randomly divided into two groups. Mice from the morphine group were injected (s.c.) with morphine in escalating doses twice per day (at 8 am and 4 pm). The escalating strategy for morphine treatment was set as 10 mg/kg on the 3rd day, 20 mg/kg on the 4th day, 30 mg/kg on the 5th day, and 40 mg/kg on the 6th day.[7,52] The mice were returned to their home cages after each morphine injection. On Day 7, the mice were injected with 40 mg/kg morphine (s.c.), and one hour later, 1 mg/kg naloxone (s.c.) was administered to induce morphine withdrawal. Immediately after naloxone administration, the mice were placed individually in the transparent box, and withdrawal signs were evaluated over the course of 30 min. Mice from the control group were given the same dose of morphine from Day 3 to Day 7, but same volume saline (s.c.) was used as the control to replace the naloxone. Jumps, paw tremors, teeth chattering (vacuous chewing), wet-dog shake, diarrhea, and loss of body weight were recorded as somatic signs of withdrawal. The body weight of the mouse was recorded before the injection of naloxone and 60 min after the injection, and the percentage of body weight loss after morphine withdrawal was used as one evaluation measurement. The number of jumps was recorded quantitatively. Teeth chattering, paw tremors, wet-dog shake, and diarrhea were evaluated over 30-second periods, with one point being given for the presence of each sign during each period. A global withdrawal score was calculated for each mouse by assigning a weighting factor to the various physical signs of withdrawal and modified as necessary.[53–56] Global withdrawal score = (number of jumps × 0.1) + (number of paw tremor × 0.1) + (number of teeth chattering ×0.1) + (number of wet-dog shakes) + (number of diarrhea × 2) + (loss of body weight percent (%) × 5). Morphine injection and behavior counting were carried out by a blinded operator.

Morphine withdrawal Conditioned Place Aversion (CPA)

The CPA test was carried out in the CPA apparatus with another group of mice. The CPA apparatus consisted of two conditioning compartments and one central connecting compartment (Figure 1A). To distinguish between the two conditioning compartments, the left ones had

walls with black-white horizontal stripes and smooth floors, while the right ones had walls with black-white vertical stripes and frosted floors. The conditioning procedure comprised a preconditioning session, four consecutive drug treatment days, one conditioning day, and one post-test day. On Day 1 and 2, all mice had free access to the entire apparatus for 15 min to reduce any effects of the experimental environment by getting the mice prepared for the following procedures. Animals with a strong initial preference for either compartment (one compartment >720 s) were eliminated from the study. To balance the CPA assay and avoid the possible effect between the two conditioning compartments, we randomly assigned any one conditioning compartment as a paired compartment for each mouse. From Day 3 to Day 7, we established the morphine withdrawal model as described in the section of naloxone-precipitated morphine withdrawal. On Day 7, the mice were confined in the paired compartments for one hour immediately after naloxone was given subcutaneously. On Day 8, mice were allowed to explore the entire apparatus for 15 min. The CPA score was defined as the time (post-paired) spent in the paired compartment minus the time (pre-paired) spent in the paired compartment. To ensure the locomotor activity of the mice remained intact before and after assigned to the paired compartment, the mice were confined in the CPA apparatus for 15 min and the mean velocity was recorded. The analysis software (JLBehv-CPPM-4, Jiliang Technology Co., Ltd., Shanghai, China) was used to record and analyze the time and moving path in two conditioning compartments.

Surgeries and stereotaxic injections

Under continuous isoflurane inhalation anesthesia, the mouse was placed in a stereotaxic frame (RWD Life Science Co., Ltd.), and body temperature was maintained at 36°C with a heating pad. After extra local analgesia with a 1 ml subcutaneous injection of 1% lidocaine above the skull, the skull was fully exposed and perforated with a stereotaxic drill at the desired coordinates relative to the bregma. Virus solution (150 nl) was infused using a microinjector with a 33G needle for ten minutes. After infusion, the needle was kept at the injection site for more than fifteen minutes before being slowly withdrawn. For viral injections and implants, the following stereotaxic coordinates were used: NAc (shell): AP: 1.09; ML: ± 0.6; DV: -4.7 were taken relative to the dura. All recombinant adeno-associated viruses (AAV) were purchased from BrainVTA Technology Corporation (Wuhan, China, Table 1).

AKAP150 knockdown

We used AAV-AKAP150 shRNA (target sequence: TCAAGAATGCTATCGAGTT) to stably conditionally knock down the expression of AKAP150 in the mice NAc. We stereotaxically injected the virus (AAV-CMV-AKAP150-shRNA-mCherry) and the corresponding control virus (AAV-CMV-AKAP150-shRNA NC-mCherry) into the NAc to conditionally knock down the expression of AKAP150 in wild-type (WT) mice. AAV-CMV-DIO-AKAP150-shRNA-mCherry along with AAV-D1-Cre-EGFP or AAV-D2-Cre-EGFP were used to specifically knock down the expression of AKAP150 in D1R-MSNs or D2R-MSNs of WT mice's NAc. We also stereotaxically injected AAV-CMV-Cre-EGFP and the corresponding control virus (CMV-EGFP) into the NAc to conditionally knock down the expression of AKAP150 in AKAP150$^{fl/fl}$ mice. AAV-D1-Cre-EGFP or AAV-D2-Cre-EGFP was used to specifically knock down the expression of AKAP150 in D1R-MSNs or D2R-MSNs of AKAP150$^{fl/fl}$ mice's NAc. AAV1 has been verified to be capable of exhibiting anterograde transsynaptic spread properties.[46] AAV1-Cre from transduced presynaptic neurons could effectively and specifically drive Cre-dependent transgene expression in selected postsynaptic neuronal targets. Therefore, we injected AAV1-TH-Cre into VTA and AAV-D1-DIO-AKAP150-shRNA or AAV-D2-DIO-AKAP150-shRNA into NAc in WT mice to explore the correlation between the VTA and expression of AKAP150 in NAc. The knockdown effectiveness in NAc was verified using western blot. The mice were kept in the cages for three weeks without any treatment after virus injection to ensure the AAV virus stable transgene expression.

Immunohistochemical (IHC) analyses

Mice were perfused with 4% paraformaldehyde under anesthesia. The brain tissues were cut into 20 μm-thick sections after 30% DEPC-sucrose dehydration at 4°C. Tissue samples used for c-fos analysis were prepared one hour after the establishment of naloxone-precipitated morphine withdrawal, and the tissue samples used for other analysis were prepared 24 hours after the establishment of morphine withdrawal. Primary antibodies against AKAP150 (Santa Cruz, Cat# sc-377055, 1:200), c-fos (Abcam, Cat#ab222699, 1:1000), TH (Merck, Cat#MAB318, 1:200) diluted in hybridization solution were then incubated with the NAc sections at 4°C overnight. The sections were subsequently incubated with fluorescein secondary antibodies with Cy3 or Alexa 488 at room temperature (approximately 26°C) for 1 hour. Finally, the sections were stained with DAPI and imaged using a confocal microscope (Nikon) equipped with a digital camera.

Western blotting

The proteins extracted from the NAc were quantified using the BCA Protein Assay kit, separated by SDS-PAGE, and transferred onto PVDF membranes. TBST with 3% skim milk was applied to block the PVDF membranes with gentle shaking at room temperature (approximately 26°C) for 1 hour to avoid nonspecific binding. Primary antibodies against β-actin (Proteintech, Cat# 66009-1, 1:5000) and AKAP150 (Santa Cruz, Cat# sc-377055, 1:200) were then used to incubate the PVDF membranes at 4°C overnight. After the membrane was rinsed three times with TBST, the membrane was incubated for 1 hour with anti-rabbit IgG secondary antibody (Abcam, ab6721, 1:10,000) at room temperature. Immunostained bands were detected using Immobilon Western Chemiluminescent HRP Substrate (Millipore, WBKLS0500) and Image Quant LAS 4000 mini system (GE Healthcare). Band intensities were analyzed using ImageJ and normalized to those of β-actin. All original western blots are shown in the supplemental information (Figure S4).

RNA extraction and real-time quantitative polymerase chain reaction (PCR)

TRIzol was used to extract total DNA from the NAc, and reverse transcription was performed following the protocol of the polymerase chain reaction (PCR) production kit (Accurate Biology, AG 11706). The primer pair of AKAP150 used for qRT-PCR was as follows: forward: 5′-AG GATGGGGCTCTTCCTAAG-3′, reverse: 5′-GGGTCTGGGCTTTTATCTCC-3′. The reaction cycle conditions were as follows: an initial denaturation at 95°C for 3 min, followed by 40 thermal cycles of 10 s at 95°C, 20 s at 58°C, and 10 s at 72°C. The ratio of mRNA expression in the NAc tissues was analyzed by the $2^{-\Delta\Delta CT}$ method.

Dendritic spine analysis

One month before establishing the morphine withdrawal model, sparsely labeled viruses Hysn-FLP: FDIO-EGFP obtained from Brain Case Biotechnology Corporation (Shenzhen, China) were injected into the mice NAc to label the morphology of the dendritic spines. We used laser confocal photography to shoot dendritic spines, took multi-layer Z-axis, and reconstructed the dendritic spine image. Spines were classified into one of the four morphological subtypes: filopodial, thin, stub, and mushroom-shaped. ImageJ was used (http://rsbweb.nih.gov/ij) to calculate the density of dendritic spines of thin, stub, and mushroom-shaped. Approximately 10 neurons selected randomly were analyzed per condition across two coverslips. The density of spines was scored in dendritic segments 10 μm in length. Finally, we counted and used the number of dendritic spines per 10 μm to describe the density of dendritic spines.

Bioinformatic analysis of ScRNA-seq data

The raw scRNA-seq data of GBM samples (GSE118918)[24] were obtained from Gene Expression Omnibus (GEO, http://www.ncbi.nlm.nih.gov/geo/) database. Codes are available on request. The R package "DoubletFinder" algorithm (https://github.com/chris-mcginnisucsf/DoubletFinder)[49] was applied to computationally detect doublets. Doublets were removed in each sample individually, with an expected doublet rate of 0.05 and default parameters used otherwise. The remaining cells survived from the doublet-detection filtering criteria were single cells. Then the R package Seurat (version 3.2.3, https://satijalab.org/seurat)[48] was used to combine and convert the expression information of the remaining cells to Seurat object. Next, the cells which had either less than 101 UMIs, or expression of less than 501 genes, or over 15% UMIs linked to mitochondrial genes were removed. Next, NormalizeData and ScaleData function of Seurat package were ran. To correct the batch effect, we integrated the scRNA-seq data for saline- (mock) and morphine- treated mice with the Harmony algorithm[50] (https://github.com/immunogenomics/harmony). We obtained cell clusters using FindCluster function of Seurat package, and visualized cells with the uniform manifold approximation and projection (UMAP) algorithm.

We annotated the cell clusters based on their average gene expression of canonical markers, including D1R-MSN (Drd1a, Pdyn, Tac1), D2R-MSN (Drd2, Penk, Adora2a), GABA_other (Gad2), ASTRO (Aldoc), OLIGOS (Cnp, Apod), Excitatory_Neuron (Cck, slc17a7), sst-Neuron (Sst, Npy), Chat-Neuron (Chat, Slc5a7), Nap1l5-Neuron (Nap1l5), Endothelial (Ly6c1), OPC (Pdgfra), Microglia (Cx3cr1), Macrophage (Mrc1), Mural (Rgs5), NSC_1 (Hmgb2), NSC_2 (Dlx1), Ependymal (Ccdc153), Erythrocyte (Hbb-bs) and VLMC (Apod, Dcn) cells consistent with the original study.[24]

QUANTIFICATION AND STATISTICAL ANALYSIS

Data were analyzed using SPSS (SPSS version 25.0, IBM, USA). All data are shown as the mean ± standard error of the mean (SEM). Data that comply with the normal distribution are compared using the two-sample independent t-test. Data that do not comply with the normal distribution are compared using the Mann-Whitney U test. The detailed statistical information is shown in Table S2. A *P*-value less than 0.05 was considered statistically significant (N.S. = no significance, $P > 0.05$; $^{*}P<0.05$; $^{**}P<0.01$; $^{***}P<0.001$).